ACS APPLIED MATERIALS & INTERFACES

Research Article

www.acsami.org

Platelet Janus Particles with Hairy Polymer Shells for Multifunctional Materials

Alina Kirillova,[†,‡] Georgi Stoychev,[†,‡] Leonid Ionov,[†,‡] Klaus-Jochen Eichhorn,[†] Mikhail Malanin,[†] and Alla Synytska*[,†,‡]

[†]Leibniz-Institut für Polymerforschung Dresden e.V., Hohe Strasse 6, D-01069 Dresden, Germany

[‡]Physical Chemistry of Polymer Materials, Technische Universität Dresden, 01062 Dresden, Germany

ABSTRACT: A novel approach is developed for the large-scale synthesis of Janus particles with platelet geometry and dense polymer shells by employing simultaneous "grafting from" of hydrophilic and hydrophobic polymers using surface-induced ATRP in emulsion. The method is based on the fabrication of an emulsion consisting of a water solution of a hydrophilic monomer and a solution of a hydrophobic monomer in an organic solvent, which is stabilized by initiator-modified kaolinite particles. Two polymers are grafted simultaneously on the opposite faces of the kaolinite particle during polymerization. The synthesized particles have a clear Janus character and are highly efficient for the stabilization of emulsions. Because of its simplicity, the method can readily be upscaled for the synthesis of large amounts of Janus particles, up to several grams.

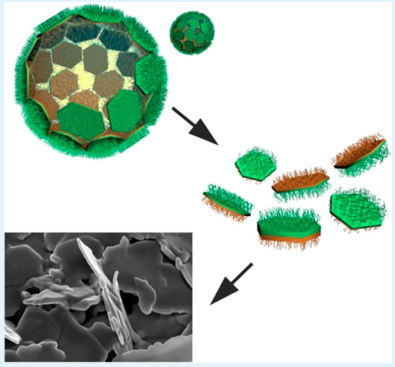

KEYWORDS: *Janus particles, kaolinite, polymer shells, hybrid hairy particles, large-scale synthesis, emulsions, anti-icing coatings*

INTRODUCTION

Janus particles are a unique kind of colloidal particles, which have different properties at opposite sides.[1−5] Because of their biphasic character, Janus particles are able to spontaneously self-organize in complex highly ordered structures and orient themselves in bulk and at interfaces,[6−12] which is particularly interesting for stabilization of emulsions and blends, design of electronic paper and novel functional coatings, synthesis, and many other applications.[3,8,13−24,42]

There are plenty of methods for the design of Janus particles using site-selective modification of particles, phase separation in block copolymers and polymer blends, site-selective crystal growth, interfacial polymerization, microfluidic jetting, etc.[25−36] According to these methods, particles with different shapes such as spheres, rods, and disks can be synthesized. Disk-like or platelet-like Janus particles are particularly interesting. For example, the energy of detachment of disk-like particles from an interface is much larger than that of rods or spheres.[37] Therefore, disks (platelets) are expected to be the most efficient for the stabilization of foams, emulsions, and polymer blends. Practically, disk-like Janus particles can be synthesized by microfluidic jetting and interfacial polymerization.[35] Kaolinite, which is a clay mineral formed by alumosilicate particles with flattened disk-like shape, is extremely abundant in nature. The diameter of kaolinite particles is ca. 1−20 μm, and the height is ca. 1 μm. There are only a few reports about the preparation and applications of kaolinite-based Janus particles. Yang et al. reported on the fabrication of inorganic silica Janus nanosheets and their Janus performance as a solid surfactant.[35] Recently, Müller et al. suggested a novel way for the synthesis of hybrid disk-like Janus particles using site-selective modification of layered-silicate kaolinites at their two opposing basal planes, the tetrahedral (TS) and the octahedral (OS) surface, which were capped by distinct functional groups.[38] The TS was selectively modified by a simple cation exchange with poly(2-(dimethylamino)ethyl methacrylate) polycations attached to a polystyrene block, while on the OS PMMA chains were covalently anchored via statistically distributed catechol groups. For this, "grafting to" approach was applied.

In this Article, we further advance the kaolinite-based approach for the large-scale synthesis of platelet Janus particles by employing simultaneously "grafting from" immobilization of hydrophilic and hydrophobic polymers by surface-induced ATRP.[43] This method allows the synthesis of hybrid Janus particles with hairy dense polymer shells in large quantities. The chemical composition and functionality as well as the density of the polymer shell can be accurately controlled during the synthesis.

EXPERIMENTAL SECTION

Materials. Ethanol abs. (EtOH, VWR, 99.9%), 3-aminopropyltriethoxysilane (APS, ABCR, 97%), hydrogen peroxide (VWR, 30%), ammonia hydroxide (Acros Organics, 28−30 wt %), α-bromoisobutyryl bromide (Aldrich, 98%), α-bromoisobutyric acid (BiBA, Aldrich, 98%), anhydrous dichloromethane (Fluka), triethylamine (Fluka), copper(II) bromide (Aldrich, 99.999%), tin(II) 2-ethylhexanoate (Aldrich, 95%), tris(2-pyridylmethyl)amine (TPMA, Aldrich, 98%), *N,N,N′,N″,N″*-

Received: May 14, 2014
Accepted: July 14, 2014
Published: July 14, 2014

pentamethyldiethylenetriamine (PMDTA, Aldrich, 99%), *N,N*-dimethylformamide (DMF, Aldrich, 99.8%), ethyl α-bromoisobutyrate (EBiB, Aldrich, 98%), toluene (Aldrich, 99.8%), chloroform (Aldrich, 99.8%), paraffin wax (mp 53−57 °C, Aldrich), anisole (Aldrich, 99%), L-ascorbic acid (Aldrich), gold(III) chloride (30 wt % in dilute HCl, Aldrich), sodium citrate dihydrate (SAFC), iodomethane (99%, Aldrich), anhydrous hexadecane (Aldrich), poly(glycidyl methacrylate) (PGMA, carboxy terminated, M_n: 48 000, Polymer Source), hydrochloric acid (HCl, 36.5−38%, Aldrich), sodium hydroxide (NaOH, pellets, Baker Analyzed Reagents), potassium chloride (KCl, Aldrich), ethylenediaminetetraacetic acid (EDTA, Aldrich), sodium bicarbonate (Fluka), and sodium dithionite (Aldrich) were used as received.

N-Isopropylacrylamide (Aldrich, 99%) was recrystallized from hexane. Lauryl methacrylate (LMA, Aldrich) and 2-(dimethylamino)-ethyl methacrylate (DMAEMA, Aldrich) were filtered prior to the polymerization through acidic, neutral, and basic aluminum oxides. Millipore water was obtained from Milli-Q (Millipore). Conductivity: 0.055 μS/cm.

Scanning Electron Microscopy (SEM). All scanning electron microscopy (SEM) images were acquired on a NEON 40 EsB Crossbeam scanning electron microscope from Carl Zeiss NTS GmbH, operating at 3 kV in the secondary electron (SE) mode. To enhance electron density contrast, samples were coated with platinum (3.5 nm) using a Leica EM SCD500 sputter coater.

Transmission Electron Microscopy (TEM) and Cryo-TEM. Transmission electron microscopy (TEM) images and cryogenic TEM images were taken with a Libra 120 cryo-TEM from Carl Zeiss NTS GmbH equipped with a LaB6 source. The acceleration voltage was 120 kV, and the energy filter with an energy window of 15 eV was used.

The kaolinite JP sample for cryo-TEM was prepared as follows. First, PDMAEMA was stained (quaternized) with CH_3I to enhance the contrast in TEM. The JPs then were dispersed in water (0.5 mg/mL) by ultrasonication for 20 min and left to settle overnight. Prior to the analysis, 3.5 μL of the sample were taken from the upper part, blotted, and vitrified in liquid ethane at −178 °C. Ultimately, an approximately 200 nm thick ice film was examined in the TEM.

Lamellas for TEM investigations were cut from kaolinite samples with a focused ion beam (FIB).

Atomic Force Microscopy (AFM). Sample preparation for AFM measurements: Kaolinite particles covered with polymers (JPs) were immobilized onto a PGMA-coated silicon wafer. For this purpose, the wafer was first washed in a mixture of hydrogen peroxide/ammonia hydroxide/water (1:1:1) to get a uniform SiO_2 layer with silanol groups. PGMA was then spin-coated onto the wafer from a 0.01% solution in $CHCl_3$ in two steps: (1) rpm = 100, time = 11 s, R/s^2 = 1900; (2) rpm = 2000, time = 31 s, R/s^2 = 1900. Afterward, the wafer was annealed for 20 min at 150 °C in a vacuum oven to chemically graft PGMA. The obtained PGMA layer thickness was 7 nm. Next, a dispersion of kaolinite JPs was prepared in chloroform (1 mg/mL), and a few drops were deposited onto a PGMA-coated wafer. The wafer was again annealed at 150 °C for 2 h in a vacuum oven. Multilayers were then removed by ultrasonication.

AFM Measurements under Water. Atomic force microscopy images were taken with a Bruker Dimension Icon AFM (Bruker, U.S.). Contact mode in fluid was used to capture force−distance curves from kaolinite samples. A Si_3N_4 cantilever with a spring constant of 0.02 N/m was used for the measurements. The "Point & Shoot" option was utilized for kaolinite samples to accurately trigger force measurements at desired locations. In this way, it could always be controlled, from which point the force curve was obtained and to which kaolinite particle (or substrate) it refers. Employing this mode, several (3−4) force curves were obtained from one single kaolinite particle to make sure of their similarity. One of the curves was then taken as a representative curve for the specific particle. Several topographical images of the sample with the respective force curves were taken for each salt concentration or pH value. Interaction forces were measured in an open fluid cell in a sealed chamber for the AFM at room temperature. Electrolyte solutions have been prepared from 0.1 M KCl, using 0.1 M HCl and KOH to adjust the pH value. Thus, measurements were carried out at pH 2, 6, and 10 in DI water and at the same pH values in 10^{-3} and 10^{-1} M KCl. The wafer was rinsed with DI water or the electrolyte solution by placing a certain amount of it (approximately 0.5−1 mL) between the sample and the probe holder with a syringe, then removing it with a tissue and placing another portion of the solution (or water). The procedure was repeated at least three times, and then the sample was left to equilibrate in the solution for 20 min. In all measurements, AFM probes were first brought into contact with the substrate. When the AFM cantilever was withdrawn from the contact, the force was measured between the probe and the sample.

Electrokinetic Measurements. The pH-dependent electrokinetic measurements (via electrophoresis) of the particles in dispersion were carried out with a ZetasizerNano ZS from Malvern Instruments Ltd. and an MPT-2 autotitrator. For all measurements, the particles were suspended in a solution of 10^{-3} M KCl in water (10 mg/24 mL or 0.42 mg/mL).The pH of the prepared suspensions was controlled by adding 0.1 M KOH or HCl aqueous solutions. Three measurements were recorded for each sample at each pH value.

Thermogravimetric Analysis (TGA). Thermogravimetric analysis (TGA) measurements have been conducted on a TGA Q5000IR device from TA Instruments Co. The chosen measurement conditions were a temperature span up to 800 °C and measurement under air.

FTIR-ATR Spectroscopy. *Qualitative Analysis.* FTIR spectra were recorded using Vertex 70 and Vertex 80v FTIR spectrometers (Bruker, Germany) equipped with DLaTGS- and MCT-detectors. To characterize the substances qualitatively, the DRIFT unit (diffuse reflectance; "Praying Mantis" (HARRICK), to characterize thin grafted polymer layers on Janus particles) or KBr-pellets preparation technique (drop casting films of initial compounds on KBr-pellets; to analyze initial substances and to find their spectral distinctions) was used. In case of KBr-preparation technique, the spectral range was 4000−400 cm^{-1} (only for DLaTGS detector), and 32 scans were coadded for every spectrum. To perform the DRIFT measurements successfully, the unit requires an MCT-detector to increase both sensitivity and signal-to-noise ratio. The spectral range in this case was 4000−600 cm^{-1}, because of MCT-detector's limitations, and 200 scans were coadded to every spectrum to obtain a reliable spectroscopic averaging. Spectral resolution was 2 cm^{-1} in all cases. A baseline correction and KBr-subtraction were carried out for every spectrum.

Quantitative Analysis. Details of the calibration procedure are given elsewhere.[39] Briefly, the grafted amount was estimated using calibration curves plotted from the absorbance spectra of the samples, made from a mixture of the polymer and particles (50 mg), as well as mixed and pressed with KBr-powder as a pellet. The spectra were recorded using spectroscopic settings similar to those for qualitative measurements. The characteristic bands at 2850 cm^{-1} (symmetric stretching vibrations of methylene group of PLMA) and 2770 cm^{-1} (symmetric stretching vibrations of methyl group coupled to amine of PDMAEMA) were used for the estimation of the grafted amount of polymers.

Optical Microscopy. Optical microscopy images were taken with an Olympus BX51 microscope equipped with an Olympus UC30 camera and recorded with analySIS docu software (Olympus Soft Imaging Solutions GmBH).

Separation and Modification of Kaolinite Particles. Kaolinite particles (Fluka) were used as received without further purification. They were separated by sedimentation in DI water for 2 days. The 100 nm to 2 μm large particles were separated using grain size separation (Atterberg method). The conventional Atterberg method was used for separating grain size fractions according to their settling velocity. After the sample was poured into a sedimentation cylinder, deionized water was added up to the desired settling height. The closed cylinder was shaken until the suspension was homogeneous. When the necessary settling time for a given equivalent diameter (e.g., 2 μm) was reached (calculated according to Stokes law), the supernatant suspension (e.g., only material <2 μm) was decanted and dried.

Purification. Kaolinite was purified after separation by the EDTA method to remove calcium- and magnesium-carbonates. Briefly, a certain amount of kaolinite particles was stirred in a 0.1 M EDTA solution for 2 h, then collected by centrifugation, washed in water several times via centrifugation/redispersion, and dried under vacuum at 60 °C. Deferration was conducted via the dithionite−citrate−bicarbonate

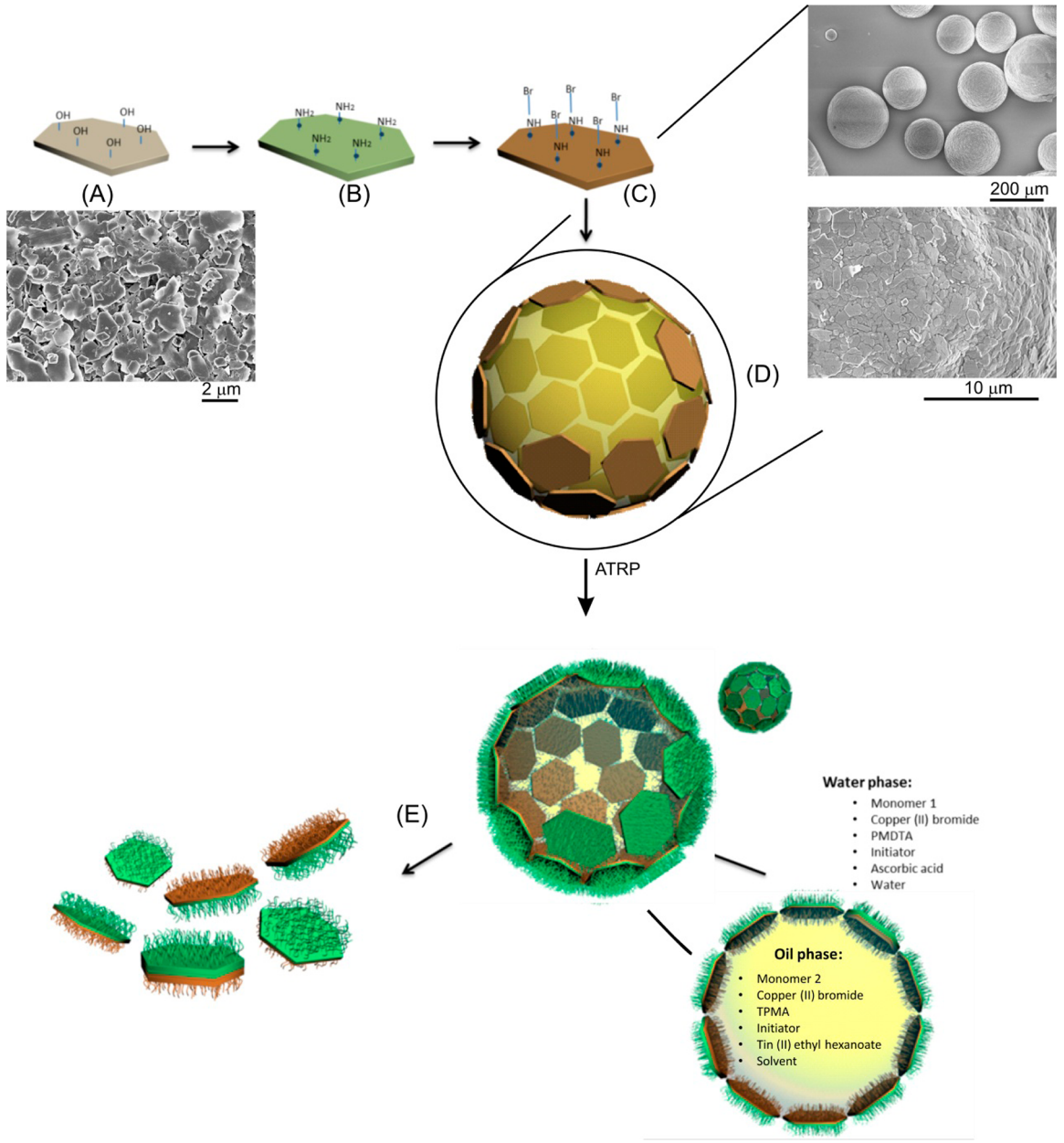

Figure 1. Scheme of a large-scale synthesis of kaolinite-based Janus particles with dense polymer shells: (A) native kaolinite particles after separation (Atterberg method) and washing; (B) kaolinite particles modified with APS; (C) kaolinite particles modified with ATRP Br-initiator; (D) emulsion droplets stabilized with premodified Br-kaolinites and representative SEM images of wax colloidosomes prepared thereof; and (E) hairy Janus particles with dense polymer shells.

(DCB) method. In short, a certain amount of kaolinite particles purified by the EDTA method was stirred in a citrate−bicarbonate solution and then heated in a water bath to 75 °C, after which dithionite was added in two portions. The mixture was allowed to stir for 10 more minutes, and the particles were then collected by centrifugation. Further, the collected particles were washed three times in the citrate−bicarbonate solution and three times in water, and then dried under vacuum at 60 °C. Purified and dried kaolinite particles were then modified with (3-aminopropyl)-triethoxysilane (APS) to introduce amino groups onto the surface. This was done by mixing the particles for 12 h in a 7.5% solution of APS in ethanol. The particles were then purified by a centrifugation/redispersion process in ethanol six times and dried in a vacuum at 60 °C.

Immobilization of the ATRP-Initiator. The ATRP-initiator (α-bromoisobutyrilbromide) is immobilized on the particle surface from its solution in dry dichloromethane (0.7 mL of BrIn in 35 mL of DCM) in the presence of triethylamine (1.4 mL). The reaction is carried out at room temperature under constant stirring for 2 h. Kaolinite particles are then purified by centrifugation/redispersion in DCM, water, and ethanol and dried under vacuum.

Grafting of Polymers Using Surface-Initiated ATRP. The polymerization of two different polymers is done simultaneously in an emulsion formed by oil in the water phase. A water-soluble monomer (DMAEMA or NIPAM) is dispersed in water, copper(II) bromide and *N*,*N*,*N*′,*N*′,*N*″-pentamethyldiethylenetriamine (PMDTA) are used as a catalyst, α-bromoisobutyric acid as an initiator in bulk, and ascorbic acid as a reducing agent. A two-neck round-bottom flask with initiator-modified kaolinite and the water-soluble ATRP mixture is put in a water bath heated to 70−80 °C and continuously purged with Ar during the whole polymerization process. The oil phase ATRP mixture consists of lauryl methacrylate as a water-insoluble monomer, anisole as a solvent, copper(II) bromide and tris(2-pyridylmethyl)amine (TPMA) as a catalyst, ethyl α-bromoisobutyrate (EBiB) as an initiator in bulk, and tin 2-ethylhexanoate as a reducing agent. This mixture is introduced to the water phase, and mixing via a mechanical stirrer is started. The

dx.doi.org/10.1021/am502973y | ACS Appl. Mater. Interfaces 2014, 6, 13106−13114

simultaneous ATRPs are conducted for 1−3 h at 1100−1400 rpm mixing speed. After polymerization, kaolinite particles are collected by centrifugation and washed in different solvents (DMF, toluene, ethanol, water).

Preparation of Monocomponent Janus Particles. Monocomponent kaolinite Janus particles with PDMAEMA and PLMA were prepared as described above, the only difference being the absence of one of the monomers. For the synthesis of PDMAEMA/Br JPs, pure anisole was taken as an oil phase, and for the synthesis of PLMA/Br JPs, pure water was used as a water phase.

Preparation of Colloidosomes with ATRP-Initiator Modified Kaolinite. Preparation of colloidosomes was done by the Pickering emulsion approach as described elsewhere.[39]Colloidosomes were prepared with kaolinite modified with the ATRP-initiator to confirm the location of the particles at the wax−water interface.

Preparation of Emulsions Stabilized with Kaolinite-Based Particles. Emulsions with nonmodified, fully covered, and Janus-type kaolinite particles were prepared, and their stability was studied over a period of 1 week. They were prepared by homogenizing water and hexadecane at room temperature for 5 min with an Ultrasonic Disintegrator UDS 751 (TOPAS GmbH) in the presence of 1 wt % of kaolinite samples. The volume fraction of hexadecane was 0.2. Samples for optical microscopy investigations were taken at once from the prepared emulsions. Camera images were then taken after certain amounts of time to investigate the stability of the emulsions.

Side-Selective Adsorption of Nanoparticles on Kaolinite-Based Particles ("Proof of Janus Character"). Gold nanoparticles (Au NPs) about 20 nm in diameter were used to selectively label the PNIPAAm- and PDMAEMA-modified region of the kaolinite JPs by coordination and electrostatic interactions, respectively. For this purpose, Au NPs were synthesized by a reduction of gold chloride, according to a procedure described elsewhere.[41] Further, samples with kaolinite JPs were prepared by dispersing 1 mg of JPs in 1 mL of the Au NPs solution (as synthesized) and diluting the dispersion with 2 additional mL of DI water. The samples were then examined with SEM.

Silica particles and poly(acrylic acid) (PAA)-covered particles (both negatively charged) with a diameter of 100 nm were used to selectively label the PDMAEMA-modified region of the kaolinite JPs through electrostatic interactions. For this purpose, silica particles and PAA-covered particles were synthesized as described elsewhere.[39] Next, 1 mg/mL dispersions were prepared by dispersing the particles in DI water. Further, 1 mg of JPs was dispersed in DI water, and 200 μL of the silica or PAA-covered particle dispersion was added slowly, while stirring. The samples were then examined with SEM.

RESULTS AND DISCUSSION

The used strategy for the synthesis of Janus particles is briefly illustrated in Figure 1. The kaolinite particles (Figure 1A) are first chemically modified to provide them functionality suitable for the initiation of the atom-transfer radical polymerization; that is, alkyl bromide groups are immobilized by sequential treatment of kaolinite particles with (3-aminopropyl) triethoxysilane (Figure 1B) and α-bromoisobutyryl bromide (Figure 1C). Next, an emulsion consisting of a water solution of a hydrophilic monomer and a solution of a hydrophobic monomer in a water-immiscible organic solvent with a mixture of initiator-modified kaolinite particles was prepared (Figure 1D). Because of their surface energy (40 mJ/m^2), which is between the surface energy of water (72 mJ/m^2) and that of oil (28 mJ/m^2), flattened kaolinite particles efficiently stabilize water−solvent emulsions because they adsorb strongly at the liquid−liquid interface. The particle can readily turn around the axis that goes through their flattened sides, while flipping of the particle is hardly possible because considerable energy excess is required. The hydrophilic and hydrophobic polymers were thus immobilized on the opposite sides of Janus particles when polymerization was started

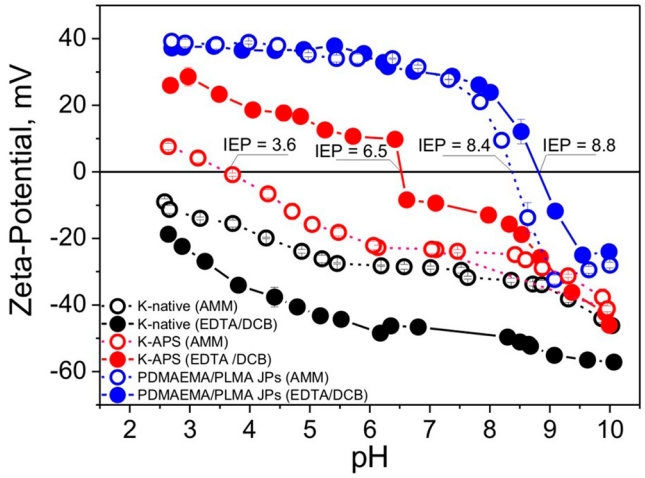

Figure 2. Zeta potential versus pH of kaolinite particles at different steps of modification. ○: Native kaolinite particles treated by ammonium−peroxide mixture (AMM). ●: Native kaolinite particles treated by EDTA and dithionite−citrate−bicarbonate (DCB) method. Red ○: APS-modified native kaolinite particles treated by ammonium−peroxide mixture. Red ●: APS-modified kaolinite particles treated by EDTA and dithionite−citrate−bicarbonate. Blue ○: Polymer-modified native kaolinite particles treated by ammonium−peroxide mixture. Blue ●: Polymer-modified kaolinite particles treated by EDTA and dithionite−citrate−bicarbonate.

in both the oil and the water phases. Finally, hairy hybrid Janus platelets with dense polymer shells were obtained (Figure 1E).

We started from the investigation of the effect of chemical treatment of kaolinite particles on the efficiency of further modification. For this, we compared the electrokinetic properties of kaolinite particles, which were treated with an ammonium−peroxide mixture (AMM, NH_4OH:H_2O_2:H_2O), with the ones purified with EDTA and dithionite−citrate−bicarbonate (DCB) method. Native kaolinite particles, independently from the purification procedure, are negatively charged over the whole range of pH values, their IEP is apparently below pH 2.5, and they are more acidic than silica dioxide (Figure 2, black curves).[39] However, the trend of the whole zeta-potential curve is more negative in the case of particles purified with EDTA/DCB (Figure 2, black curve, solid circles) as compared to those washed with AMM mixture (Figure 2, black curve, empty circles). Treatment with amino-silane dramatically shifts the IEP into the basic region (IEP = 6.5) (Figure 2, red curve, solid circles) if particles were previously treated with EDTA/DCB. On the other hand, shift of the IEP after modification with amino-silane of the particles washed with the AMM mixture is moderate (IEP = 3.6) and does not approach the IEP of a silicon wafer modified with the same silane (IEP = 8.0). Moreover, the zeta potential of Janus particles synthesized using AMM is smaller than that of Janus particles made using the EDTA/DCB procedure (Figure 2, blue curves). Therefore, EDTA/DCB treated particles were used for the next immobilization of α-bromoisobutiryl bromide.

Polymerization of methyl methacrylate on initiator-modified kaolinite particles using ARGET-ATRP[40] was performed to determine the number of available initiator sites and grafting density. We added a small amount of a free initiator to the monomer solution and assumed that the molecular weight of the polymer obtained in solution is comparable to that of grafted polymer chains. The molecular weight of the polymer in solution obtained by GPC was M_n = 76 800; M_w = 250 000 g/mol. The amount of grafted polymer determined by TGA was 20 wt %.

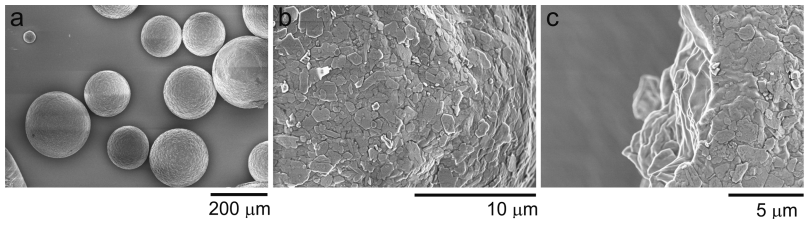

Figure 3. Representative SEM images of paraffin colloidosomes prepared from Br−In-modified kaolinite particles and wax.

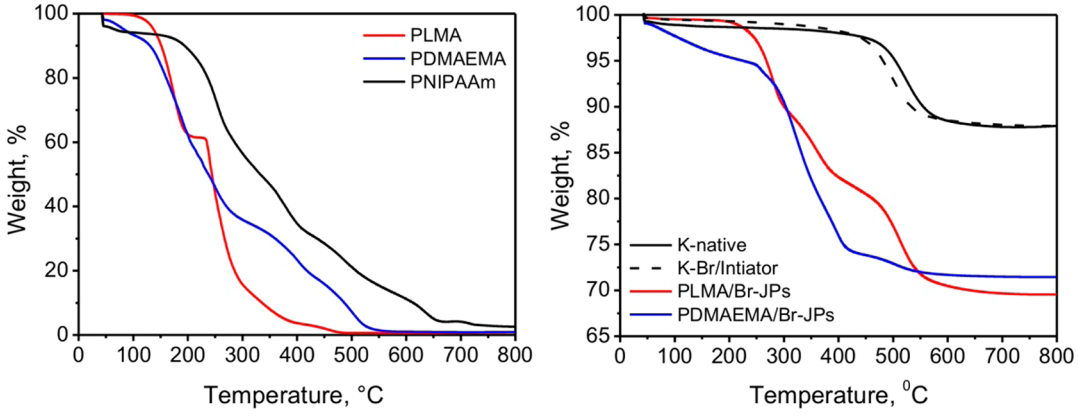

Figure 4. TGA curves of pure polymers (left) and monocomponent Janus particles PDMAEMA/Br-JPs and PLMA/Br-JPs (right).

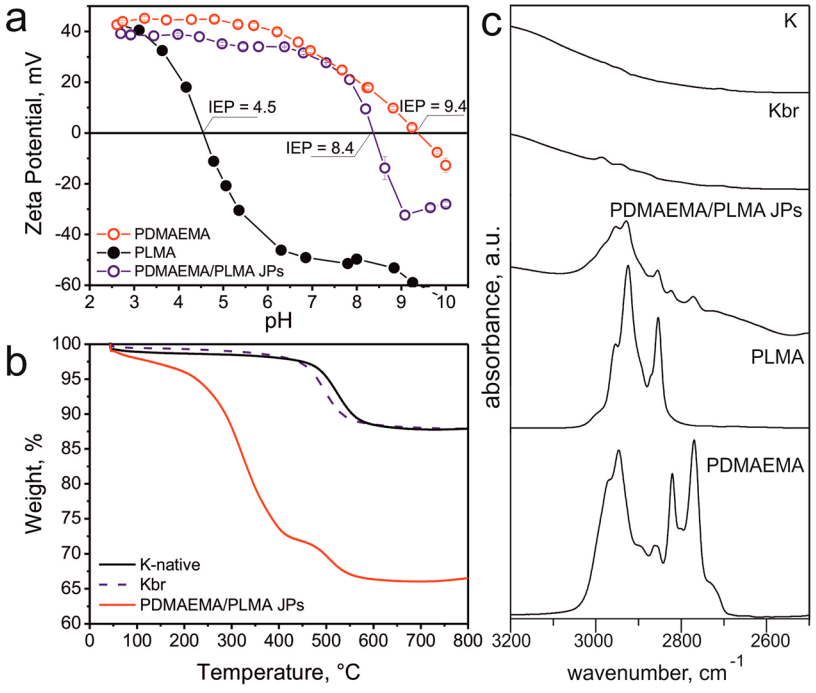

Figure 5. Properties of homogeneous and Janus particles. (a) Zeta potential (red line, PDMAEMA-modified particles; black line, PLMA-modified particles, blue line, PDMAEMA/PLMA JPs); (b) TGA (black line, native kaolinite particles; blue line, kaolinite with bromo-initiator, Kbr; red line, PDMAEMA/PLMA JPs); and (c) FTIR spectra (K, native kaolinite; Kbr, kaolinite particles with bromo-initiator for ATRP, PDMAEMA/PLMA JPs, PLMA, and PDMAEMA as pure polymers).

The grafting density was determined by considering the surface area of kaolinite particles, which was determined by BET measurements to be S_{BET} = 22.276 m^2/g. The estimated value of grafting density was ca. 0.11 chains/nm^2 that is comparable to the previously reported value of grafting density obtained using AGRET-ATRP on a SiO_2 substrate.

$$\Gamma\ (\text{chains/nm}^2) = \frac{f_{pol}}{1 - f_{pol}} \frac{N_A}{M_n S_{BET}} \quad (1)$$

We investigated the behavior of Br-modified kaolinites at the water−oil interface. This experiment was done using paraffin as a high melting point oil. The Br-modified kaolinites were mixed with molten paraffin; the obtained blend was mixed with water

dx.doi.org/10.1021/am502973y | ACS Appl. Mater. Interfaces 2014, 6, 13106−13114

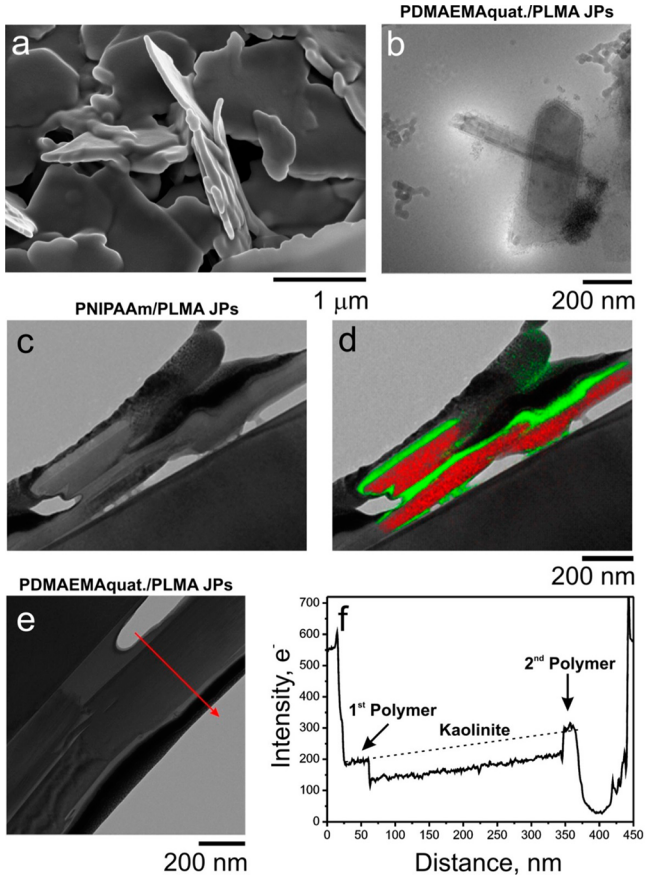

Figure 6. Electron microscopy investigation of kaolinite Janus particles: (A) scanning electron microscopy and (B) cryo-TEM image of PDMAEMA/PLMA-JPs; PDMAEMA was quaternized by methyl iodide for better contrast; (C,D) TEM and EFTEM images of a PNIPAM/PLMA Janus particle FIB lamella; red and green are the signals of oxygen and carbon, respectively; (E) TEM image of a FIB lamella of a Janus kaolinite particle; and (F) intensity profile along the red arrow in (E).

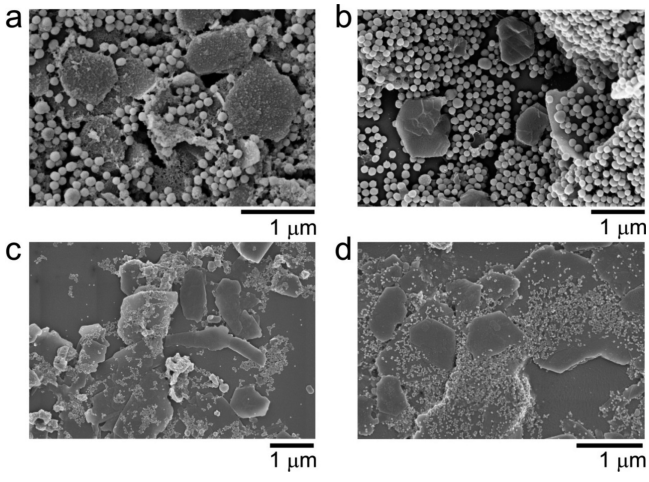

Figure 7. Side-selective adsorption of PAA NPs on (a,b) PDMAEMA/PLMA Janus particles and Au NPs on (c) PDMAEMA/PLMA-JPs and (d) PNIPAM/PLMA-JPs.

and finally cooled. Use of the high melting point oil allows SEM investigation of kaolinite particles at room temperature. It was found that paraffin droplets have spherical shape with the size of 50−200 μm after cooling to room temperature and crystallization of the oil (Figure 3). The surface of the obtained paraffin (wax) droplets is fully covered by flattened kaolinite particles, which form a monolayer (Figure 3c). This behavior can be fully explained by considering the surface tension of water, oil, and Br-modified particles, which are 72, 28, and 40 mJ/m^2, respectively. The surface tension of Br-modified particles is between the values of surface tensions of liquids, and, therefore, their segregation between liquids is energetically favorable.

Next, we performed separate site-selective grafting of hydrophilic and hydrophobic monomers. For this purpose, Br-modified particles were added to an emulsion of anisole in a water solution of DMAEMA (hydrophilic monomer) and, in another experiment, to an emulsion of LMA (hydrophobic monomer) in water. The mass loss, as measured by TGA, in both cases is ca. 30% (Figures 4 and 5). Considering that only one-half of each kaolinite disc is modified by grafted polymer chains, the thicknesses of grafted layers are found (using eq 2) to be ca. 40 nm. Therefore, on the basis of the values of the distance between the grafting sites and the shell thickness, the polymer layer can be considered to be in the brush regime.

$$H\ (\mathrm{nm}) = \frac{2f_{\mathrm{pol}}}{\rho_{\mathrm{pol}} S_{\mathrm{BET}} (1 - f_{\mathrm{pol}})} \qquad (2)$$

In the next step, we performed simultaneous grafting of hydrophilic (2-(dimethylamino)ethyl methacrylate, DMAEMA) and hydrophobic (lauryl methacrylate, LMA) monomers from the emulsion. The obtained particles were thoroughly characterized using electrophoresis, TGA, and FTIR spectroscopy. The isoelectric point (IEP) of PDMAEMA/PLMA Janus particles was found to be at IEP = 8.4 that is between the values of IEP of fully covered particles with the same polymers ($\mathrm{IEP}_{\mathrm{PDMAEMA}}$ = 9.9; $\mathrm{IEP}_{\mathrm{PLMA}}$ = 4.4) (Figure 5a). This is an indication of a successful grafting of two polymers. The value of the IEP of Janus particles, however, does not allow an estimation of the composition (ratio between both polymers on one Janus particle) because the polymers have different swelling properties (PDMAEMA is a polyelectrolyte and is highly swollen in water; PLMA is hydrophobic and does not swell in water), and their contribution to the total charge of particles can hardly be estimated. We also synthesized PNIPAM-PLMA Janus particles using a similar approach.

Further, the grafted amount of PDMAEMA and PLMA was estimated using TGA and FTIR spectroscopy (Figure 5b,c). The mass loss measured by TGA in the case of bicomponent Janus particles was comparable to the mass loss of monocomponent Janus particles (Figure 4), meaning that the thickness of polymer layers is 2 times smaller, that is, 20 nm. It was found that FTIR spectra of Janus particles contain characteristic bands of both polymers: PLMA (at 2850 cm^{-1}) and PDMAEMA (at 2770 cm^{-1}); therefore, it is the direct evidence for successful grafting of both polymers. We estimated the ratio between two polymers using a calibration curve obtained from FTIR spectra of a polymer mixture with different composition. It was found that the ratio between PDMAEMA and PLMA in Janus particles is PDMAEMA:PLMA = 4.3:5.7; that is, Janus particles are symmetric. Therefore, on the basis of TGA and FTIR results, one can conclude that the thickness of each polymer layer is ca. 20 nm and the layers are in brush regime.

The microscopic investigation of the synthesized Janus particles was performed to further prove the successful grafting of polymers. Polymer-modified particles have a smoother surface

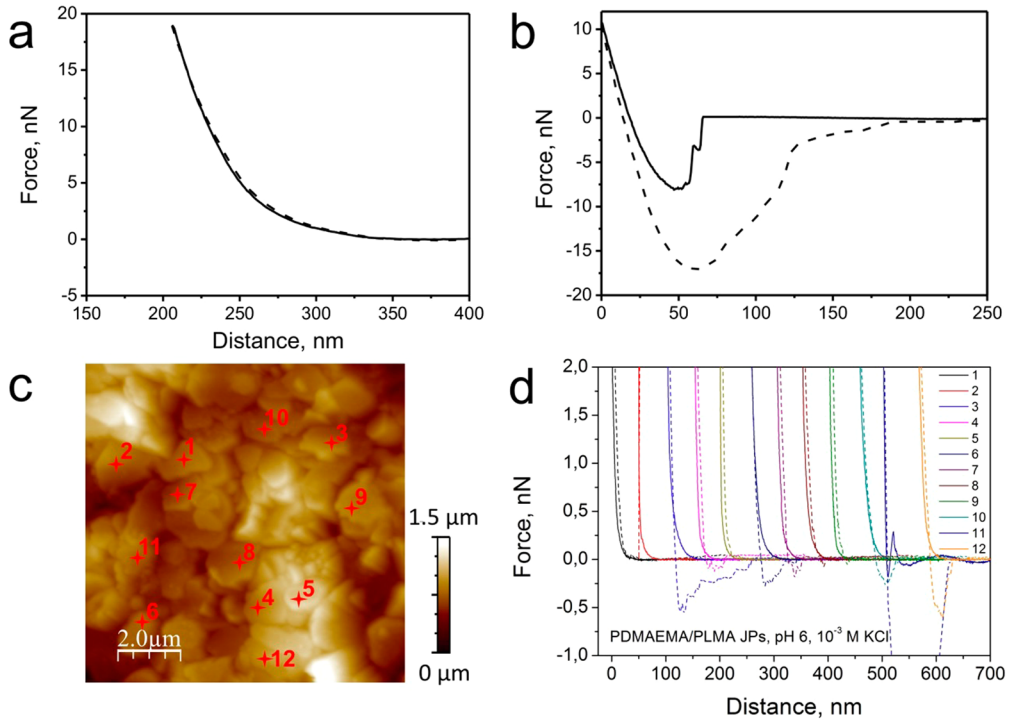

Figure 8. Force measurements on PDMAEMA/PLMA Janus particles. (a,b) Force−distance curves obtained on pure PDMAEMA and PLMA surfaces, respectively; (c) topography images of Janus particles; and (d) force−distance curves of selected Janus particles.

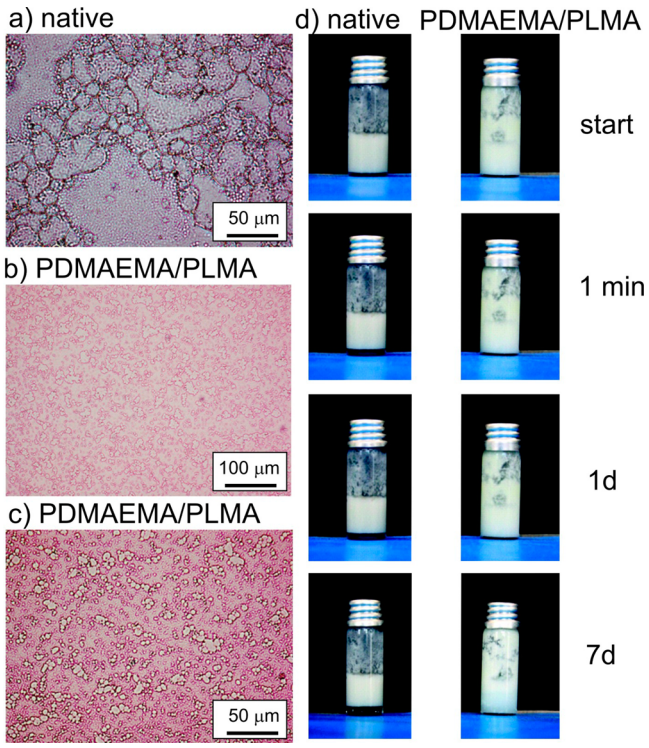

Figure 9. Stabilization of a water−oil emulsion by native kaolinites and PDMAEMA/PLMA Janus particles. (a) Microscopy image of the emulsion stabilized by native kaolinite particles after 15 min; (b,c) microscopy image of the emulsion stabilized by Janus kaolinite particles after 15 min; and (d) photo shapshots of emulsions stabilized by native kaolinite particles and Janus particles after different amounts of time (as prepared, after 1 min, 1 day, and 7 days).

(Figure 6a) than the native ones because of the polymer shell. One can also see, using cryo-TEM, the shell of the swollen in water quaternized-PDMAEMA (the polymer was quaternized by CH_3I for better contrast) around the PDMAEMA/PLMA Janus particles (Figure 6b). The contrast between the different phases of PNIPAM/PLMA Janus particles was investigated using TEM and EFTEM methods. One can distinguish between the inorganic core with its strong oxygen signal, and the polymer shell with its strong carbon signal (Figure 6c,d). We could also observe contrast between quaternized-PDMAEMA and PLMA sides (Figure 6e,f): the polymer shell on one side of the particle is darker (PDMAEMA) than on the other (PLMA). The thickness of each layer evaluated using TEM images was found to be in the range of ca. 30 nm, which is comparable to the results of TGA and FTIR. Thus, on the basis of scanning and transmission electron microscopy observations, we can conclude that the grafting of polymers to both sides of kaolinite particles was successful.

Moreover, we further proved the Janus character of synthesized particles by side-selective adsorption of negatively charged PAA-coated SiO_2 particles onto PDMAEMA/PLMA Janus particles as well as adhesion measurements. In particular, we observed that PAA-coated SiO_2 particles adsorb not on all kaolinite particles. Some of the particles remain absolutely uncoated. The observed effect can readily be explained by considering properties of each polymer: PLMA is hydrophobic and uncharged; PDMAEMA is hydrophilic and positively charged; PAA is hydrophilic and negatively charged. PAA particles are strongly electrostatically stabilized and do not adsorb on any hydrophobic as well as hydrophilic uncharged or negatively charged surface. On the other hand, PAA particles are strongly adsorbed on the positively charged PDMAEMA surface due to electrostatic attraction. Therefore, the character of adsorption of PAA particles can be considered as an indication of the grafted polymer: PDMAEMA sides of Janus particles are

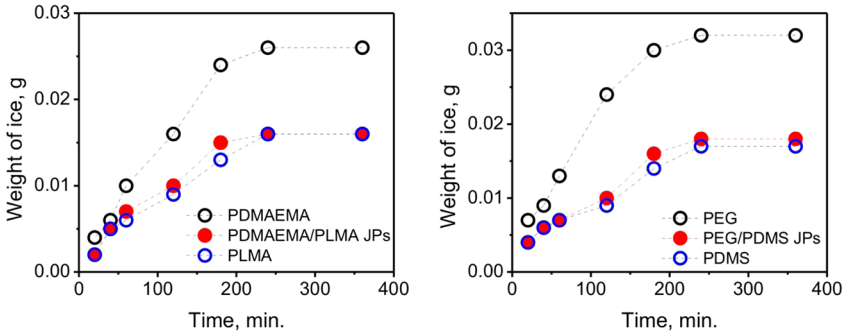

Figure 10. Kinetics of ice formation on PDMAEMA and PLMA flat surfaces, and PDMAEMA/PLMA JPs (left); PEG and PDMS flat surfaces, and PEG/PDMS JPs (right).

covered by PAA particles, while PLMA ones are bald (Figure 7a,b). Similar experiments with side-selective adsorption were performed with Au nanoparticles (negatively charged, ZP = −35 mV) on quaternized PDMAEMA/PLMA-Janus particles (Figure 7c) as well as PNIPAM/PLMA-JPs (Figure 7d). In both cases, Au NPs are selectively adsorbed onto either the PDMAEMA or the PNIPAM side.

AFM force measurements in aqueous conditions at controlled pH and ionic strength confirm different properties of opposite sides of bicomponent Janus particles (Figure 8). The grafted polymers PLMA and PDMAEMA have different adhesive properties. In particular, PDMAEMA is nonadhesive (Figure 8a), while PLMA is strongly adhesive (Figure 8b). We performed test force measurements of Janus particles adsorbed on a silica wafer (totally, more than 20 Janus particles were tested in each image; representative experiment is shown in Figure 8c). It was found that one-half of them are absolutely nonadhesive and another one-half are adhesive (adhesion force is ca. 0.3−0.5 nN), which is an indication of the different properties of opposite sides of Janus particles (Figure 8d).

Finally, we demonstrated an application of amphiphilic PDMAEMA/PLMA Janus particles for the stabilization of water−oil emulsions and the design of coatings with anti-icing properties.

Stabilization of Emulsions. It was found that liquid droplets stabilized by PDMAEMA/PLMA Janus particles are much smaller than droplets stabilized by unmodified kaolinite. Moreover, the amphiphilic PDMAEMA/PLMA Janus particles are more efficient for the stabilization of an emulsion than native kaolinite: the emulsion with Janus particles remains stable for 7 days, while the emulsion with native particles starts to separate after 1 min (Figure 9).

Anti-Icing Surfaces. Furthermore, the application field for the synthesized Janus particles can be extended toward anti-icing coatings. For this purpose, PDMAEMA/PLMA JPs and PEG/PDMS (polyethylene glycol-polydimethylsiloxane) JPs were tested and compared to flat surfaces with the same polymers (Figure 10). Kinetics of frost formation was measured in a chamber, where temperature and humidity were controlled (under 80% of relative humidity, temperature range from +20 °C to −20 °C, cooling rate 0.5 °C using Peltier-Element). Notably, the curves for Janus particles are between those for pure polymers, indicating the amphiphilic character of the Janus particles. Moreover, surfaces made of amphiphilic (hydrophobic/hydrophilic) Janus particles combine low freeze point of hydrophilic polymeric surfaces and low adhesion of the ice intrinsic to hydrophobic surfaces. The results on the investigation of the anti-icing behavior on coatings made of Janus particles will be published soon.

CONCLUSIONS

We developed a novel approach for the large-scale synthesis of hairy platelet Janus particles with polymeric shells. The method is based on the fabrication of an emulsion consisting of water and oil solutions of hydrophilic and hydrophobic monomers, which is stabilized by initiator-modified kaolinite particles. The advantage of this approach is its simplicity and the possibility of the synthesis of large amounts of Janus particles at once that is the main limitation of photolithography, which was also used for fabrication of platelet-like Janus particles.[44,45] The proposed approach can be applied to various surfaces with disc-like or platelet geometry and, hence, can aid in the design of advanced functional materials for different technological applications such as stabilization of emulsions, and the design of anti-icing or antifouling coatings.

AUTHOR INFORMATION

Corresponding Author

*Tel.: +49 (0351) 4658 327. Fax: +49 (0351) 4658 474. E-mail: synytska@ipfdd.de.

Notes

The authors declare no competing financial interest.

ACKNOWLEDGMENTS

We are thankful to Dr. P. Formanek for the assistance with electron microscopy, M. Göbel for preparing the FIB lamellas, K. Arnhold for TGA, A. Caspari for zeta potential measurements, and Dr. A. Dreschler for the assistance with the AFM measurements. DFG (grant SY 125/4-1) is acknowledged for financial support.

REFERENCES

(1) Walther, A.; Müller, A. H. E. Janus Particles. *Soft Matter* **2008**, *4*, 663−668.

(2) Lee, K. J.; Yoon, J.; Lahann, J. Recent Advances with Anisotropic Particles. *Curr. Opin. Colloid Interface Sci.* **2011**, *16*, 195−202.

(3) Walther, A.; Müller, A. H. E. Janus Particles: Synthesis, Self-Assembly, Physical Properties, and Applications. *Chem. Rev.* **2013**, *113*, 5194−5261.

(4) Wurm, F.; Kilbinger, A. F. M. Polymeric Janus Particles. *Angew. Chem., Int. Ed.* **2009**, *48*, 8412−8421.

(5) Jiang, S.; Chen, Q.; Tripathy, M.; Luijten, E.; Schweizer, K. S.; Granick, S. Janus Particle Synthesis and Assembly. *Adv. Mater.* **2010**, *22*, 1060−1071.

(6) Chen, Q.; Whitmer, J. K.; Jiang, S.; Bae, S. C.; Luijten, E.; Granick, S. Supracolloidal Reaction Kinetics of Janus Spheres. *Science* **2011**, *331*, 199−202.
(7) Chen, Q.; Bae, S. C.; Granick, S. Staged Self-Assembly of Colloidal Metastructures. *J. Am. Chem. Soc.* **2012**, *134*, 11080−11083.
(8) Synytska, A.; Ionov, L. Stimuli-Responsive Janus Particles. *Part. Part. Syst. Charact.* **2013**, *30*, 922−930.
(9) Chen, Q.; Bae, S. C.; Granick, S. Directed Self-Assembly of a Colloidal Kagome Lattice. *Nature* **2011**, *469*, 381−384.
(10) Li, W.; Gunton, J. D. Self-Assembly of Janus Ellipsoids II: Janus Prolate Spheroids. *Langmuir* **2013**, *29*, 8517−8523.
(11) Liu, Y.; Li, W.; Perez, T.; Gunton, J. D.; Brett, D. Self-Assembly of Janus Ellipsoids. *Langmuir* **2011**, *28*, 3−9.
(12) Ren, B.; Ruditskiy, A.; Song, J. H.; Kretzschmar, I. Assembly Behavior of Iron Oxide-Capped Janus Particles in a Magnetic Field. *Langmuir* **2011**, *28*, 1149−1156.
(13) Lv, W.; Lee, K. J.; Li, J.; Park, T.-H.; Hwang, S.; Hart, A. J.; Zhang, F.; Lahann, J. Anisotropic Janus Catalysts for Spatially Controlled Chemical Reactions. *Small* **2012**, *8*, 3116−3122.
(14) Yoon, J.; Kota, A.; Bhaskar, S.; Tuteja, A.; Lahann, J. Amphiphilic Colloidal Surfactants Based on Electrohydrodynamic Co-jetting. *ACS Appl. Mater. Interfaces* **2013**, *5*, 11281−11287.
(15) Ruhland, T. M.; Gröschel, A. H.; Ballard, N.; Skelhon, T. S.; Walther, A.; Müller, A. H. E.; Bon, S. A. F. Influence of Janus Particle Shape on Their Interfacial Behavior at Liquid−Liquid Interfaces. *Langmuir* **2013**, *29*, 1388−1394.
(16) Zhao, Y.; Gu, H.; Xie, Z.; Shum, H. C.; Wang, B.; Gu, Z. Bioinspired Multifunctional Janus Particles for Droplet Manipulation. *J. Am. Chem. Soc.* **2013**, *135*, 54−57.
(17) Yong, X.; Crabb, E. J.; Moellers, N. M.; Balazs, A. C. Self-Healing Vesicles Deposit Lipid-Coated Janus Particles into Nanoscopic Trenches. *Langmuir* **2013**, *29*, 16066−16074.
(18) Gao, W.; Pei, A.; Dong, R.; Wang, J. Catalytic Iridium-Based Janus Micromotors Powered by Ultralow Levels of Chemical Fuels. *J. Am. Chem. Soc.* **2014**, *136*, 2276−2279.
(19) Gao, W.; Pei, A.; Feng, X.; Hennessy, C.; Wang, J. Organized Self-Assembly of Janus Micromotors with Hydrophobic Hemispheres. *J. Am. Chem. Soc.* **2013**, *135*, 998−1001.
(20) Baraban, L.; Streubel, R.; Makarov, D.; Han, L.; Karnaushenko, D.; Schmidt, O. G.; Cuniberti, G. Fuel-Free Locomotion of Janus Motors: Magnetically Induced Thermophoresis. *ACS Nano* **2012**, *7*, 1360−1367.
(21) Kaewsaneha, C.; Tangboriboonrat, P.; Polpanich, D.; Eissa, M.; Elaissari, A. Janus Colloidal Particles: Preparation, Properties, and Biomedical Applications. *ACS Appl. Mater. Interfaces* **2013**, *5*, 1857−1869.
(22) Chen, Q.; Yan, J.; Zhang, J.; Bae, S. C.; Granick, S. Janus and Multiblock Colloidal Particles. *Langmuir* **2012**, *28*, 13555−13561.
(23) Synytska, A.; Khanum, R.; Ionov, L.; Cherif, C.; Bellmann, C. Water-Repellent Textile via Decorating Fibers with Amphiphilic Janus Particles. *ACS Appl. Mater. Interfaces* **2011**, *3*, 1216−1220.
(24) Berger, S.; Ionov, L.; Synytska, A. Engineering of Ultra-Hydrophobic Functional Coatings Using Controlled Aggregation of Bicomponent Core/Shell Janus Particles. *Adv. Funct. Mater.* **2011**, *21*, 2338−2344.
(25) Nie, L.; Liu, S. Y.; Shen, W. M.; Chen, D. Y.; Jiang, M. One-Pot Synthesis of Amphiphilic Polymeric Janus Particles and Their Self-Assembly into Supermicelles with a Narrow Size Distribution. *Angew. Chem., Int. Ed.* **2007**, *46*, 6321−6324.
(26) Walther, A.; Hoffmann, M.; Müller, A. H. E. Emulsion Polymerization Using Janus Particles as Stabilizers. *Angew. Chem., Int. Ed.* **2008**, *47*, 711−714.
(27) Kim, H.; Carney, R. P.; Reguera, J.; Ong, Q. K.; Liu, X.; Stellacci, F. Synthesis and Characterization of Janus Gold Nanoparticles. *Adv. Mater.* **2012**, *24*, 3857−3863.
(28) Zhao, N.; Gao, M. Magnetic Janus Particles Prepared by a Flame Synthetic Approach: Synthesis, Characterizations and Properties. *Adv. Mater.* **2009**, *21*, 184−187.
(29) Lattuada, M.; Hatton, T. A. Preparation and Controlled Self-Assembly of Janus Magnetic Nanoparticles. *J. Am. Chem. Soc.* **2007**, *129*, 12878−12889.
(30) Shah, R. K.; Kim, J.-W.; Weitz, D. A. Janus Supraparticles by Induced Phase Separation of Nanoparticles in Droplets. *Adv. Mater.* **2009**, *21*, 1949−1953.
(31) Pradhan, S.; Xu, L.; Chen, S. Janus Nanoparticles by Interfacial Engineering. *Adv. Funct. Mater.* **2007**, *17*, 2385−2392.
(32) Chen, Y.; Nurumbetov, G.; Chen, R.; Ballard, N.; Bon, S. A. F. Multicompartmental Janus Microbeads from Branched Polymers by Single-Emulsion Droplet Microfluidics. *Langmuir* **2013**, *29*, 12657−12662.
(33) Hu, J.; Zhou, S.; Sun, Y.; Fang, X.; Wu, L. Fabrication, Properties and Applications of Janus Particles. *Chem. Soc. Rev.* **2012**, *41*, 4356−4378.
(34) Li, J.; Wang, L.; Benicewicz, B. C. Synthesis of Janus Nanoparticles via a Combination of the Reversible Click Reaction and "Grafting to" Strategies. *Langmuir* **2013**, *29*, 11547−11553.
(35) Liang, F.; Shen, K.; Qu, X.; Zhang, C.; Wang, Q.; Li, J.; Liu, J.; Yang, Z. Inorganic Janus Nanosheets. *Angew. Chem., Int. Ed.* **2011**, *50*, 2379−2382.
(36) Ling, X. Y.; Phang, I. Y.; Acikgoz, C.; Yilmaz, M. D.; Hempenius, M. A.; Vancso, G. J.; Huskens, J. Janus Particles with Controllable Patchiness and Their Chemical Functionalization and Supramolecular Assembly. *Angew. Chem., Int. Ed.* **2009**, *48*, 7677−7682.
(37) Nonomura, Y.; Komura, S.; Tsujii, K. Adsorption of Disk-Shaped Janus Beads at Liquid-Liquid Interfaces. *Langmuir* **2004**, *20*, 11821−11823.
(38) Weiss, S.; Hirsemann, D.; Biersack, B.; Ziadeh, M.; Müller, A. H. E.; Breu, J. Hybrid Janus Particles Based on Polymer-Modified Kaolinite. *Polymer* **2013**, *54*, 1388−1396.
(39) Berger, S.; Synytska, A.; Ionov, L.; Eichhorn, K. J.; Stamm, M. Stimuli-Responsive Bicomponent Polymer Janus Particles by "Grafting from"/"Grafting to" Approaches. *Macromolecules* **2008**, *41*, 9669−9676.
(40) Matyjaszewski, K.; Dong, H.; Jakubowski, W.; Pietrasik, J.; Kusumo, A. Grafting from Surfaces for "Everyone": ARGET ATRP in the Presence of Air. *Langmuir* **2007**, *23*, 4528−4531.
(41) Frens, G. Controlled Nucleation for the Regulation of the Particle Size in Monodisperse Gold Suspensions. *Nature (London), Phys. Sci.* **1973**, *241*, 20−22.
(42) Synytska, A.; Bellmann, C.; Ripperger, S.; Schnitzler, K.; Cherif, C.; Lehmann, B. Funktionalisierung von textilien Flächengebilden, ein Verfahren zu ihrer Herstellung und Verwendung. Ger. Offen. DE102010028662A1, Nov 10, 2011.
(43) Synytska, A.; Kirillova, A. Janus Particles with Polymer Shells. Eur. Pat. Appl. EP 3173-X-29502, 2014.
(44) Lyubarskaya, Y. L.; Shestopalov, A. A. Multicomponent Inorganic Janus Particles with Controlled Compositions, Morphologies, and Dimensions. *ACS Appl. Mater. Interfaces* **2013**, *5*, 7323−7329.
(45) Clark, T. D.; Ferrigno, R.; Tien, J.; Paul, K. E.; Whitesides, G. M. Template-Directed Self-Assembly of 10-μm-Sized Hexagonal Plates. *J. Am. Chem. Soc.* **2002**, *124*, 5419−5426.